Multitemp 2015

Comparison between spatial and temporal estimation of entropy on polarimetric SAR images

Flora Weissgerber[1,2], Elise Colin-Koeniguer[2], Nicolas Trouvé[2] and Jean-Marie Nicolas[1]

[1]Telecom Paristech - [2]Onera

23/07/2015

Classification using PolSAR images

Classification : a long term task for PolSAR

- Lots of algorithms :
  - Freeman-Durden decomposition [Freeman and Durden, 1998]
  - Yamagushi decomposition [Yamaguchi et al., 2005]
  - Touzi decomposition [Touzi, 2007]
  - ...
- **H/α/A decomposition** [Cloude and Pottier, 1997]
  $\rightarrow$ Building / Non-Building discrimination

Times Series are now available !

- New satellites
- New image distribution policy

New tools ?

Outlines

SAR and PolSAR

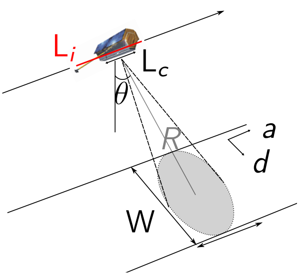

L_i : integration length

L_c : physical length

θ : incidence angle

R : target-radar distance

W : swath width

(a,d) : azimuth axis, distance axis

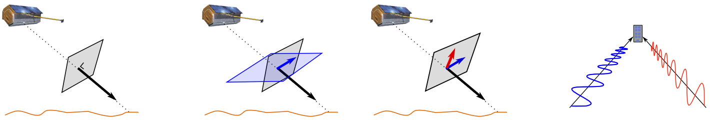

Propagation vector **k**   Polarization H   Polarization V   Polarization H and V

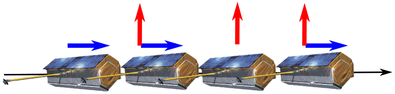

Alternate emission of H and V
Simultaneous reception of H and V

3 information channels : HH , HV=VH, VV

Speckle and Covariance Matrix

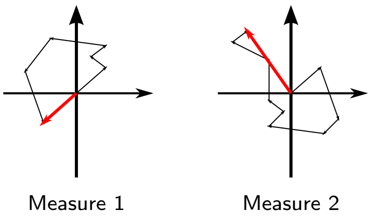

$\mathbf{p} \in \mathbb{C}^M$, a pixel of image $\mathbf{I}$ [Goodman, 1976] :

$$P(\mathbf{p}\,;\mathbf{C}) = \frac{1}{\pi^M |\mathbf{C}|} e^{-\mathbf{p}^\dagger \mathbf{C}^{-1} \mathbf{p}}$$

$\mathbf{C}$: covariance matrix

$$\mathbf{C} = E[\mathbf{p}\mathbf{p}^\dagger] \rightarrow \tilde{\mathbf{C}} = \frac{1}{L} \sum_{l=1}^{L} \mathbf{p}_l \mathbf{p}_l^\dagger$$

Spatial averaging

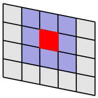

1 image : L neighbouring pixels

Temporal averaging

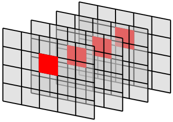

L images : 1 pixel

Adaptative averaging

NL-SAR
[Deledalle et al., 2014]
Binary partition trees
[Alonso-Gonzalez et al., 2012]

Definition

Eigenvalue and Eigenvector of $\tilde{\mathbf{C}}$:

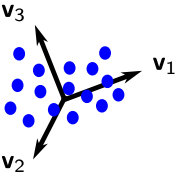

$\{\mathbf{v}_l\}_{l=1,M}$: eigenvectors of $\tilde{\mathbf{C}}$
principal components

$\{\lambda_l\}_{l=1,M}$: associated eigenvalue
variance associated to the component

Polarimetric Entropy :

$$\mathrm{H} = -\sum_{k=1}^{M} p_k \log_M p_k \qquad p_k = \frac{\lambda_k}{\sum_{l=1}^{M} \lambda_l}$$

Measure of the variability in the samples set :

$\mathrm{H} = 0$ — $p_1 = 1, p_2 = p_3 = 0$

$\mathrm{H} = 0.6309$ — $p_1 = p_2 = \frac{1}{2}, p_3 = 0$

$\mathrm{H} = 1$ — $p_1 = p_2 = p_3 = \frac{1}{3}$

Under-estimation of H

Influence of the number of samples :

- $L \geq 3$
- L small : H under-estimated [López-Martínez et al., 2005]

$$\mathrm{H} = 0.309, \ \mathrm{H} = 0.4, \ \mathrm{H} = 0.69$$

6 pixels

$P(H|H)\ P(H|H)\ P(H|H)$

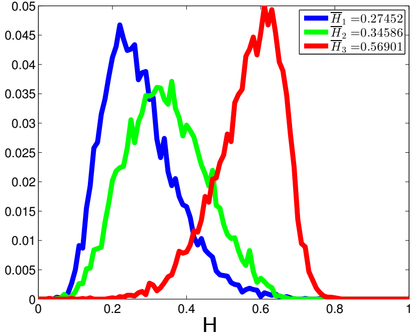

$$\overline{\mathrm{H}} = 0.28, \ \overline{\mathrm{H}} = 0.35, \ \overline{\mathrm{H}} = 0.57$$

100 pixels

$P(H|H)\ P(H|H)\ P(H|H)$

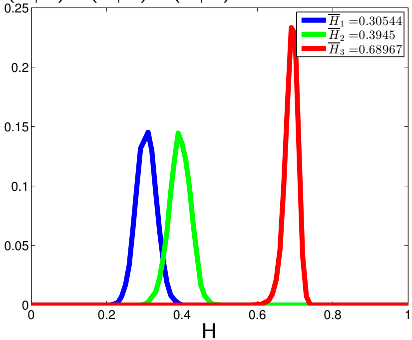

$$\overline{\mathrm{H}} = 0.30, \ \overline{\mathrm{H}} = 0.40, \ \overline{\mathrm{H}} = 0.69$$

Over-estimation of H

Noise

H $\nearrow$ CNR $\searrow$ clutter to noise ratio

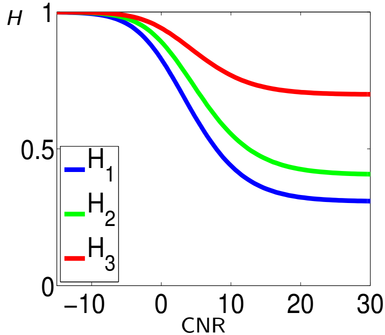

$\mathbf{p} = \boldsymbol{\tau} \circ \mathbf{s} + \mathbf{b}$

$\mathbf{T} = \mathbf{C} + \mathbf{\Gamma}$

$\mathbf{\Gamma} = \sigma_b^2 \boldsymbol{I}_d$: entropy $= 1$

Mixing

H $\nearrow$ when mixing

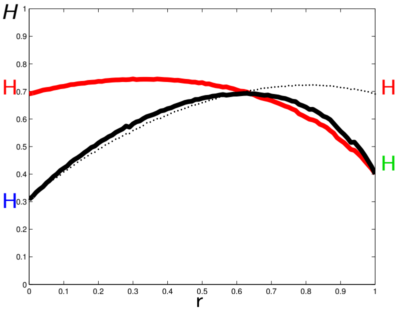

Entropy estimated using 100 pixels from 2 populations with the mixing-proportion r :

- $r\,\mathcal{N}(0, \mathbf{C}_2)$ et $(1 - r)\,\mathcal{N}(0, \mathbf{C}_1)$
- $\cdot\cdot$ $r\,\mathcal{N}(0, \mathbf{C}_3)$ et $(1 - r)\,\mathcal{N}(0, \mathbf{C}_1)$
- $r\,\mathcal{N}(0, \mathbf{C}_2)$ et $(1 - r)\,\mathcal{N}(0, \mathbf{C}_3)$

City of San Francisco

Neighbourhood with particular street orientation

Map : SoMa District

Ikonos image

Data sets

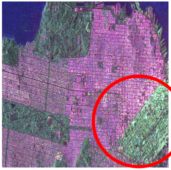

SoMa District **Candlestick point**

RADARSAT 2
C : 5mx8m
1 image

TerraSAR-X DRA
X : 6mx2m
3 images

UAVSAR
L : 1.8mx0.8m
12 images

Entropy in low resolution

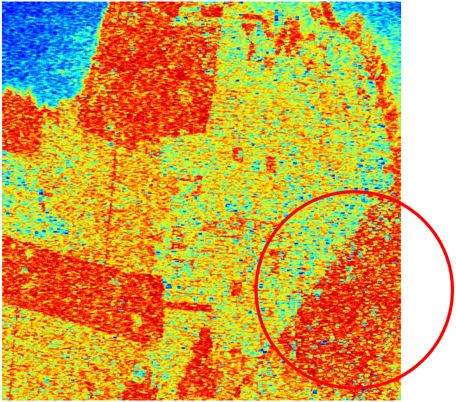

Entropy on Radarsat-2 image, C band, 5mx8m resolution : 5×5 boxcar filter

- Good contrast between vegetation and parallel oriented neighbourhood
- High entropy on SoMa district

Entropy in high resolution

TerraSAR-X , X band, 6mx2m resolution

- Entropy varies in time (especially for the sea)
- Poor contrast : mixing phenomenon

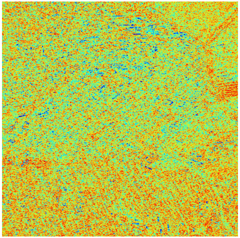

2010-04-11

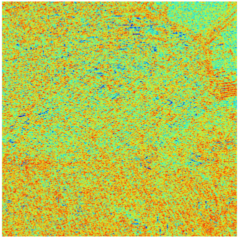

2010-04-22

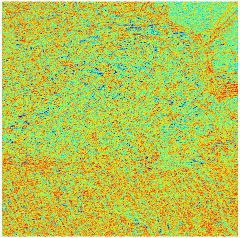

2010-05-03

3×9 boxcar filter

Entropy in temporal series

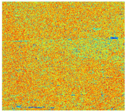
2009-02-18

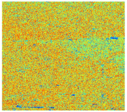
2009-11-19

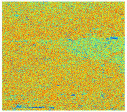
2010-01-15

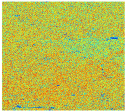
2010-03-01

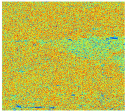
2010-04-23

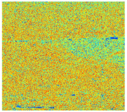
2010-11-10

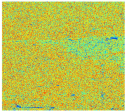
2011-11-03

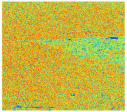
2012-04-18

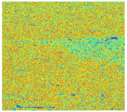
2012-11-02

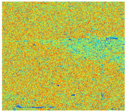
2013-05-07

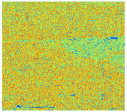
2014-06-20

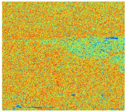
2014-11-12

3×4 boxcar filter

H 0  1

- Entropy varies in time
- Poor contrast : mixing phenomenon
- SoMa District (oriented 0° from track) small entropy

Temporal Entropy

Pauli color image

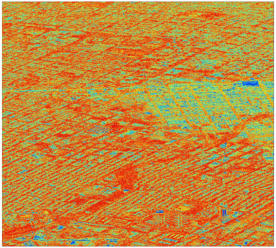

Temporal entropy

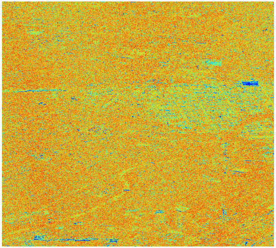

Spatial entropy 2009-02-18

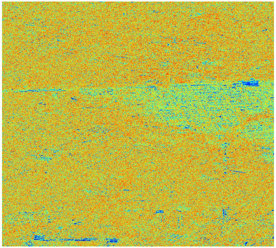

Spatial entropy 2010-04-23

H 0  1

Spatial entropy in temporal series

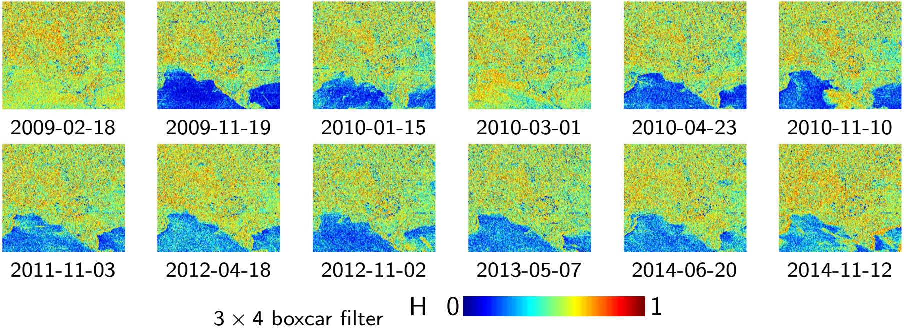

- Entropy varies in time
- Poor contrast : mixing phenomenon

Temporal Entropy

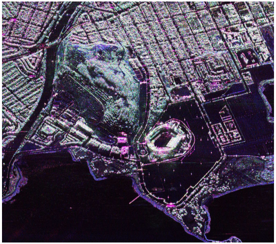

Pauli color image

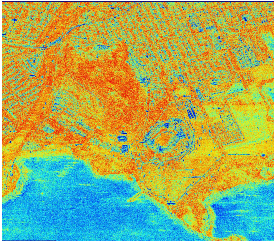

Temporal entropy

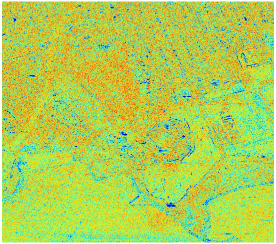

Spatial entropy 2009-02-18

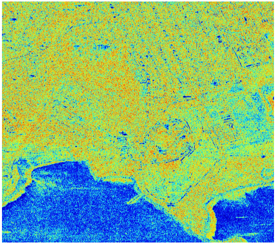

Spatial entropy 2010-04-23

H 0  1

4 entropy behaviours

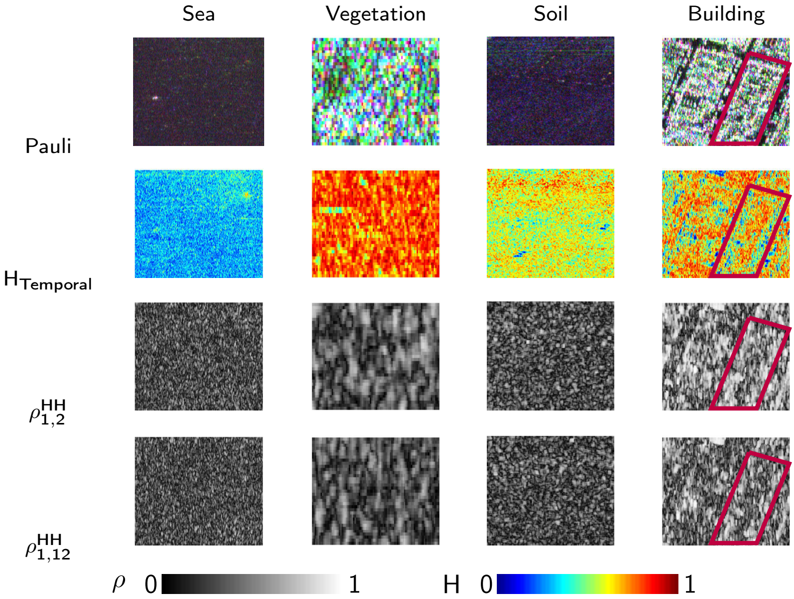

Polarimetric time-series

- numerous spatial entropy maps
- one temporal entropy map

Complementary information

- Spatial entropy
  - spatial disorder : variation of scattering mechanism between neighbour pixels
  - poor contrast in high resolution (mixing during the estimation)
- Temporal entropy
  - temporal disorder : variation of scattering mechanism in time
  - no resolution loss
  - add information on the degree of coherence
    - high and stable degree of coherence $\rightarrow$ low entropy
    - decreasing degree of coherence $\rightarrow$ medium entropy
    - low degree of coherence $\rightarrow$ various entropy

In the future

- Study the temporal α/A maps
- Combine these information into a classifier
- Take into account the orientation of the building

Bibliographie

- Alonso-Gonzalez, A., Lopez-Martinez, C., and Salembier, P. (2012).
  Filtering and Segmentation of Polarimetric SAR Data Based on Binary Partition Trees.
  IEEE Transactions on Geoscience and Remote Sensing, 50(2) :593–605.
- Cloude, S. R. and Pottier, E. (1997).
  An Entropy Based Classification Scheme for Land Applications of Polarimetric SAR.
  IEEE Transactions on Geoscience and Remote Sensing, 35(1) :68–78.
- Deledalle, C.-A., Denis, L., Tupin, F., Reigber, A., and Jäger, M. (2014).
  NL-SAR : a unified Non-Local framework for resolution-preserving (Pol)(In)SAR denoising.
  IEEE Transactions on Geoscience and Remote Sensing, 4(53) :2021 – 2038.
- Freeman, A. and Durden, S. L. (1998).
  A Three-Component Scattering Model for Polarimetric SAR Data.
  IEEE Transactions on Geoscience and Remote Sensing, 36(3) :963–973.
- Goodman, J. W. (1976).
  Some fundamental properties of speckle.
  Journal of the Optical Society of America, 66(11) :1145–1150.

Bibliographie (cont.)

- López-Martínez, C., Pottier, E., and Cloude, S. R. (2005).
  Statistical Assessment of Eigenvector-Based Target Decomposition Theorems in Radar Polarimetry.
  IEEE Transactions on Geoscience and Remote Sensing, 43(9) :2058–2074.
- Touzi, R. (2007).
  Target Scattering Decomposition in Terms of Roll-Invariant Target Parameters.
  IEEE Transactions on Geoscience and Remote Sensing, 45(1) :73–84.
- Yamaguchi, Y., Moriyama, T., Ishido, M., and Yamada, H. (2005).
  Four-Component Scattering Model for Polarimetric SAR Image Decomposition.
  IEEE Transaction on Geoscience and Remote Sensing, 43(8) :1699–1706.